Sequel of the IMPROVE Project: petrographic analysis of the concrete from concrete prims tests

Isabel Fernandes [(1)], António Santos Silva [(2)], Violeta Ramos [(3)], Dora Soares [(4)]

(1) Instituto Dom Luiz (IDL), Faculdade de Ciências, Universidade de Lisboa, Campo Grande, 1749–016, Lisboa, Portugal, mifernandes@fc.ul.pt

(2) National Laboratory for Civil Engineering, Lisboa, Portugal, ssilva@lnec.pt

(3) Camborne School of Mines, University of Exeter, Penryn Campus, Cornwall, UK and Instituto de Ciências da Terra, Pólo Porto, Portugal, v.i.monteiro-ramos@exeter.ac.uk

(4) National Laboratory for Civil Engineering, Lisboa, Portugal, dsoares@lnec.pt

Abstract

IMPROVE Project (2012-2015) is aimed at studying the alkali-reactivity of Portuguese aggregates, including innocuous, slowly-reactive and normally-reactive aggregates collected all over the country. The granitic samples were the most numerous, considering the fact that several important concrete structures have been constructed with these aggregates for decades and an increasing number is showing manifestations of alkali-silica reaction (ASR) since the 1990s.

The aggregates were characterized by petrographic methods before being submitted to concrete prism tests (CPT) under 38 ºC for 1 year and 60 ºC for 20 weeks.

After the conclusion of the expansion tests, thin sections were produced for identification of the minerals and/or textures in the aggregates which might have caused ASR and to recognise the main microscopic features originated in concrete when submitted to such aggressive environmental conditions.

In the present work, several samples were selected from each of the classes of potential reactivity according with the petrographic characterization of the aggregates. The petrographic classification is compared with the results of expansion obtained in the CPT and a rating is made regarding the features observed in the concrete thin sections, namely the cracks developed and the distribution of ASR gel, aiming to find a possible correlation with the expansion values observed for the two test conditions used.

Keywords: *alkali-silica gel; petrography; reactive silica; strained quartz*

1. INTRODUCTION

The most commonly used aggregates in Portugal are granite, limestone and sand from alluvial deposits in the Mainland and basalts in the islands. The studies on deterioration of concrete due to deleterious internal reactions started in late 1980's with the analysis of concrete from structures showing manifestations compatible with alkali-silica reactions (ASR) and delayed ettringite formation (DEF) [1]. Since then, the number of structures identified as showing cracking, exudation, deformation of structural elements and misalignments has increased dramatically [2, 3, 4, 5]. The petrographic analysis of concrete from damaged structures typically shows that cracks initiate in the interior of the reactive aggregate particles and then extend to the cement paste leading to the expansion of concrete. The cracks are usually empty in the interior of the aggregate particles and the reaction products occur close to the interfaces with the cement paste but are more abundant in the cracks that cross the cement paste. Several studies have been focusing on the composition and structure of the gel which results from ASR, which is predominantly amorphous. However, crystalline ASR compounds can be also found, namely lamellar, rosette-like or acicular crystals [6]. The ASR products composition, with Si, Ca, K and Na and, in some cases, Al, is quite variable. Si is the main component [7, 8] and the gel contains always an unknown number of molecules of water. The composition of a crystalline ASR product does not correspond to a stoichiometric mineral but there have been many attempts to associate the composition and texture with a number of minerals such as okenite [9], cryptophyllite-rhodesite and mountainite-shlykovite [10], mountainite and rhodesite [11], and shlykovite [12].

Alkali-carbonate reaction (ACR), the term used to name the reaction between concrete's alkaline pore solution and certain argillaceous dolomitic limestones, is not fully explained and some authors have concluded that carbonate rocks are reactive when they combine dedolomitization and the presence of micro- to cryptocrystalline quartz, regarding ACR as a form of ASR [13]. ASR was detected in Portugal in a concrete structure using limestone with cryptocrystalline quartz in nodules [1]. However, cracking occurs in concrete using carbonate rocks containing no or very low content of silica

and further research is needed to clarify the ACR mechanism.

IMPROVE project, financed by the Foundation for Science and Technology (Fundação para a Ciência e a Tecnologia – FCT), was carried out between 2012 and 2015, aiming at the characterization of the potential reactivity to alkalis of the Portuguese aggregates most commonly used in the manufacture of concrete. The characteristics of some of the granitic and basaltic aggregates and the results obtained from the expansion tests performed were already published elsewhere [14,15,16].

In the project, more than 80 samples were studied. The tests performed for the characterization of the aggregates followed the methodology recommended both in RILEM AAR-0 [17] and the national standards [18], namely:

- petrographic analysis of aggregates under optical microscope,
- concrete prism tests (CPT), using two different conditions of exposure namely RILEM AAR-3.1 and RILEM AAR-4.1 [17].

Most of the Portuguese aggregates are classified as Class II or reactivity uncertain [17] and as slowly/late-reactive in accordance with Lindgård et al. [19,20], creating expansive reactions 15 to 20 years after construction of the structures. Components such as the silica polymorphs and opal are quite unusual to inexistent in the country. However, in 2015 at least 13 large concrete dams and 14 bridges were listed with different degrees of deterioration in Portugal. One large dam was demolished and replaced by a new one in 2015.

In what concerns the granitic samples, and taking into account the national experience with these aggregates, the Portuguese recommendation LNEC E 461 [18] was followed: the CPT must be always performed whatever the result of the petrographic analysis.

The CPT results show that most of the samples exhibit values of expansion well below the threshold of potential reactivity in both tests and just a few overcame the standard limits considered [15,16]. Some of the aggregates were classified as reactive in one of the tests but not on the other and the correlation between the petrographic analysis and the values of CPT expansion are acceptable only for intensely deformed rocks (deformed granites) and for those samples containing micro- to cryptocrystalline quartz (natural gravel and one severely strained meta-rhyolite).

The present work summarizes the results obtained with three main goals: to correlate the classification by petrographic assessment with the results of the CPTs; to identify which components of the aggregates are associated with manifestations of ASR in the concrete prisms; to compare the texture and the composition of the reaction products with those usually found in ASR affected structures. The study was performed using an optical microscope and a scanning electron microscope (SEM), complemented by the qualitative chemical analysis of ASR products using Energy Dispersive Spectroscopy (EDS). The data obtained in the petrographic study of the concrete thin sections is compared with the CPT expansion results.

2. MATERIALS AND METHODS

In IMPROVE Project a total of 81 samples was collected throughout the country, in the Mainland, Azores and Madeira Islands. A summary is presented in Table 2.1. The aggregates are divided according with the origin in a quarry or in a natural deposit, as the variability of the lithology found in the batches preparing for concrete manufacture is much higher in polymictic gravel deposits than in quarries. In the group of quarries, the aggregates are divided in large sets concerning mainly the mineral composition and texture, such as e.g. in granite *s.l.* and in basalt *s.l.*, including a range of compositions. The sample of amphibolite was included as it showed to be a challenging aggregate [21].

Samples of crushed rock were collected in the quarries from batches ready to be sold as aggregate for concrete. The samples collected in unconsolidated deposits were as far as possible representative of the batches used for concrete manufacture. The average weight of each sample sent to the laboratory was of about 100 kg. In the quarries, also blocks of rock were selected for the study of the mineral composition and texture.

Table 2.1: Summary of the type and number of samples tested in the Project.

Origin	Lithology	Abbreviation	Number of samples
Quarry	Granite *s.l.* (granite, granodiorite)	GR	36
	Gabbro-diorite and meta-rhyolite	DT	2
	Basalt *s.l.* (basalt, trachybasalt, basanite, basanitoid)	BS	18
	Amphibolite	AF	1
	Quartzite	QZ	4
	Limestone	CL	11
	Dolomite	DL	3
Natural gravel	Reactive polymictic gravel	BR	6

The petrographic study of all the aggregates followed RILEM AAR-1.1 [17] and 1.2 [22] and the Portuguese specification LNEC E 461 [18]:

- Class I—very unlikely to be alkali-reactive
- Class II—potentially alkali-reactive or alkali-reactivity uncertain
- Class III—very likely to be alkali-reactive

The difference between Class I and II was established regarding the content of microcrystalline silica obtained by point-counting, with classification as innocuous when this content is lower than 2%. Class III in AAR-0 criteria is limited to aggregates containing opal or opaline silica, which does not occur with the aggregates tested and is almost inexistent in Portugal. Therefore, Class II was subdivided according with [19] in slowly and normally-reactive.

The samples were crushed and sieved to obtain the grain sizes proportions recommended for the CPT. The concrete prisms were prepared using a CEM I 42,5R [23] with alkalis content ranging from 0.86 to 0.89%. The alkali content of all manufactured concrete was 5.5 $Na_2O_{equiv.}/m^3$. The concrete prisms were exposed to different conditions [17]:

- long term concrete prism test AAR-3.1, at 38 ºC for 1 year,
- accelerated concrete prism test AAR-4.1, at 60 ºC for 20 weeks.

At the completion of the tests, each concrete prism was cut lengthwise and then slices taken from the middle of the prisms with 10x25x50 mm^3 sent for the production of thin sections. For each prism, one thin-section was analysed, with the largest dimension of the thin section parallel to the length of the prism and collected close to the top of the prism.

For the study of the manifestation of ASR in the concrete prisms, a selection was made from the samples available, divided according to the petrographic classification. Concrete petrography followed the indications in Poole and Sims [24]. For the quantification of the manifestations of ASR, the principles used in the Damage Rating Index [e.g. 25] were followed, in this analysis designated by micro-DRI, as it was obtained on thin sections. The thin sections were analyzed under a Leica DM750 P polarizing microscope coupled with a Leica ICC50 HD camera for photomicrographic record. The polished thin sections were sputter-coated with carbon under vacuum in a VG MICROTECH E6700/T800 instrument for analysis in a JEOL JSM-6301F scanning electron microscope instrument, equipped with a field-emission gun (FEG) and a NORAN VOYAGER energy dispersive spectrometer (EDS).

3. RESULTS

3.1 Petrographic analysis of aggregates

The petrographic analysis of the aggregates allowed the classification in the three groups regarding the potential reactivity to alkalis. Samples were selected covering the three classes, namely:

- Non-reactive/innocuous aggregates: basalts *s.l.* (BS7, BS8 and BS9); limestone (CL3) and dolomite (DL3) (Figure 3.1a and b);

- Slowly-reactive aggregates and aggregates of uncertain reactivity: most of the granitic samples (GR1, GR3, GR4, GR5, GR6, GR7, GR8, GR9, GR10, GR14, GR17 and GR20), one basalt containing volcanic glass (BS6), one diorite (DT2), two dolomite samples (DL1 and DL2) and one sample of limestone containing microcrystalline quartz and clasts of quartz (CL4) (Figure 3.1c and d);
- Normally-reactive aggregates: those containing intensely strained and/or micro- to cryptocrystalline quartz; selected samples are the natural gravel (BR2), the meta-rhyolite (DT1) (Figure 3.1e), three deformed granites (GR2, GR13, GR18) (Figure 3.1f) and the amphibolite sample (AF).

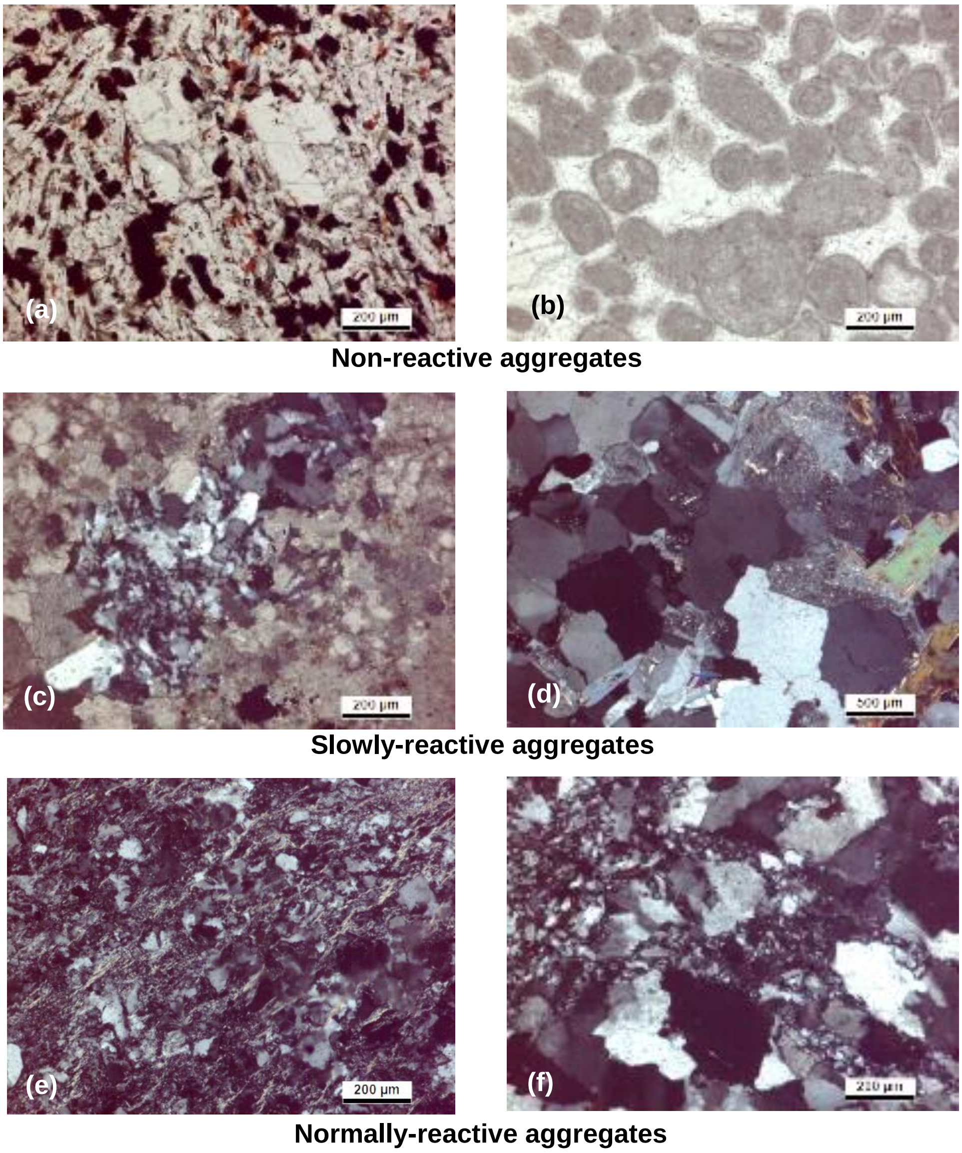

Figure 3.1: Examples of the textures identified in the samples tested: a) basalt (BS7); b) limestone (CL3); c) siliceous dolomite (DL1); d) non-deformed granite (GR14); e) meta-rhyolite (DT1); f) deformed granite with subgraining (GR18).
Photomicrographs a) and b) in PPL; all the others in XPL.

Basalts *s.l.* vary in grain size and slightly in mineral composition. The samples analysed do not contain (rhyolitic) volcanic glass or polymorphs of silica (free silica), supposed to cause ASR when volcanic rocks are used, except BS6 in which altered volcanic glass was identified.

Some of the samples of limestone and dolomite show stylolite features highlighted by clay minerals and iron oxides in consequence of diagenetic stresses, but no quartz was identified. The great majority of

Portuguese limestone do not contain any clasts of quartz nor microcrystalline silica and are classified as innocuous. However, the quarry of the sample CL4 shows heterogeneous composition and in some of the particles included in the thin sections scarce clasts of quartz or microcrystalline quartz were identified. These aggregates were classified “of reactivity uncertain”, adopting a conservative approach regarding the potential reactivity.

The granitic *s.l.* and the diorite (DT2) samples classified as slowly-reactive, as listed above, contain abundant quartz but no deformation signs or subgraining are visible under the microscope. The amphibolite sample contains scarce microcrystalline quartz in veinlets and cracks with cataclastic infilling.

All the samples that exhibit components with intense deformation were classified as normally-reactive. These cover the polymictic gravel (BR), which contains quartzite/sandstone mainly composed of grains of quartz exhibiting sutured boundaries, sedimentary overgrowth and solution-deposition features due to diagenetic and/or tectonic stresses, but also cataclastic rock fragments, phyllite and schist with microcrystalline quartz. The dolomite DL1, in which micro- to cryptocrystalline quartz was identified, and the diorite (DT1), intensely deformed and containing abundant micro- to cryptocrystalline quartz were included in this class. In normally-reactive class also the granitic rocks with gneissic features were included, exhibiting crystals of quartz with undulatory extinction, strain lamellae, ribbons, bulging and subgraining. Mica and feldspar crystals are usually bent in these rocks.

3.2 Concrete Prism Tests (CPT)

Following the petrographic analysis, concrete prism tests AAR-3.1 and AAR-4.1 were performed. For the classification of the aggregates regarding the results of the laboratory expansion tests the following thresholds were used (RILEM AAR-7.3) [17]:

- RILEM AAR-3.1 – expansion >0.030% at 1 year of test
- RILEM AAR-4.1 – expansion >0.030% at 20 weeks of test

Table 3.1 presents the results obtained for each aggregate.

3.3 Petrographic analysis of the concrete thin sections

The petrographic analysis of the thin sections prepared from the concrete prisms at the end of the testing period exhibits a quite variable intensity of the features related to ASR. The features observed under microscope are listed:

- De-bonding of the aggregate particles from the cement paste (without gel)
- Gel in the interfaces of aggregate particles with the cement paste
- Cracks crossing coarse aggregate particles: open (empty) or containing ASR gel
- Cracks running through de cement paste: open or containing ASR gel
- Cracks cutting fine aggregate particles: open or containing ASR gel
- Rims of reaction in the cement paste of particles of limestone and dolomite
- ASR gel in voids

Figure 3.2 illustrates the main ASR manifestations identified under optical microscope. The manifestations of ASR are scarce and very discrete to absent for all the aggregates classified as innocuous by the petrographic analysis.

The concrete petrography analysis shows that the number of manifestations of ASR and their distribution in the concrete are associated with the particles of aggregate with deformation, for the granitic samples, as already concluded in Ramos et al. [16], and on the presence of subgraining and micro- to cryptocrystalline quartz.

This analysis confirmed that the most reactive aggregates are: the deformed meta-rhyolite with abundant cryptocrystalline quartz (DT1); the natural gravel (BR); and the deformed granites with subgraining, namely GR2, GR13 and GR18.

Table 3.1: Classification of the potential reactivity of the aggregates regarding petrography and the results of the concrete prism tests (NR – non-reactive; R – reactive).

<table>
<tr><th rowspan="2">Samples</th><th rowspan="2">Petrography</th><th colspan="2">AAR-3.1</th><th colspan="2">AAR-4.1</th></tr>
<tr><th>Expansion (%)</th><th>Classification</th><th>Expansion (%)</th><th>Classification</th></tr>
<tr><td>BS7</td><td rowspan="5">Innocuous</td><td>0.03</td><td rowspan="4">NR</td><td>0.01</td><td rowspan="4">NR</td></tr>
<tr><td>BS8</td><td>0.02</td><td>0.01</td></tr>
<tr><td>CL3</td><td>0.03</td><td>0.02</td></tr>
<tr><td>DL3</td><td>0.02</td><td>0.01</td></tr>
<tr><td>BS9</td><td>0.03</td><td>R</td><td>0.02</td><td>NR</td></tr>
<tr><td>BS6</td><td rowspan="18">Slowly-reactive</td><td>0.02</td><td rowspan="6">NR</td><td>0.00</td><td rowspan="6">NR</td></tr>
<tr><td>DL1</td><td>0.00</td><td>0.02</td></tr>
<tr><td>GR5</td><td>0.01</td><td>0.02</td></tr>
<tr><td>GR6</td><td>0.01</td><td>0.02</td></tr>
<tr><td>GR7</td><td>0.02</td><td>0.02</td></tr>
<tr><td>GR9</td><td>0.00</td><td>0.01</td></tr>
<tr><td>DT2</td><td>0.01</td><td rowspan="6">NR</td><td>0.03</td><td rowspan="6">R</td></tr>
<tr><td>GR1</td><td>0.02</td><td>0.03</td></tr>
<tr><td>GR3</td><td>0.02</td><td>0.04</td></tr>
<tr><td>GR4</td><td>0.00</td><td>0.04</td></tr>
<tr><td>GR10</td><td>0.02</td><td>0.06</td></tr>
<tr><td>GR14</td><td>0.02</td><td>0.03</td></tr>
<tr><td>CL4</td><td>0.03</td><td>R</td><td>0.02</td><td>NR</td></tr>
<tr><td>DL2</td><td>0.03</td><td rowspan="5">R</td><td>0.03</td><td rowspan="5">R</td></tr>
<tr><td>GR8</td><td>0.06</td><td>0.05</td></tr>
<tr><td>GR17</td><td>0.04</td><td>0.05</td></tr>
<tr><td>GR19</td><td>0.03</td><td>0.03</td></tr>
<tr><td>GR20</td><td>0.04</td><td>0.05</td></tr>
<tr><td>AF</td><td rowspan="6">Normally-reactive</td><td>0.03</td><td rowspan="6">R</td><td>0.07</td><td rowspan="6">R</td></tr>
<tr><td>BR</td><td>0.08</td><td>0.14</td></tr>
<tr><td>DT1</td><td>0.14</td><td>0.21</td></tr>
<tr><td>GR2</td><td>0.06</td><td>0.06</td></tr>
<tr><td>GR13</td><td>0.08</td><td>0.09</td></tr>
<tr><td>GR18</td><td>0.03</td><td>0.04</td></tr>
</table>

In the quantification of signs of ASR following the criteria in [25] a selection was made in what concerns the features that are observed but do not point out to deleterious ASR. In Figure 3.3 the most important are presented, namely: gel partially or totally filling voids (Figure 3.3a), several fine cracks in the cement paste that did not show any relation with the characteristics of the aggregates or originated from the interior of the aggregate particles (Figure 3.3b), artefacts created during the production of the thin sections such as debonding, thinning of the cement paste and pull-outs (Figure 3.3c).

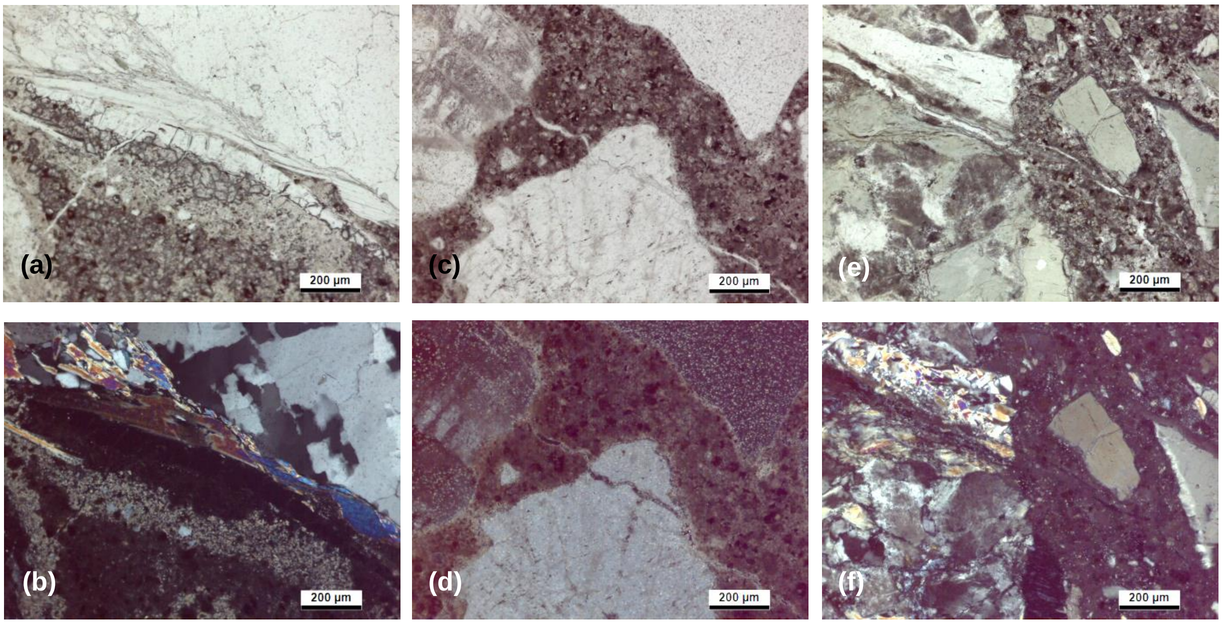

Figure 3.2: ASR features observed in the thin sections of the concrete prisms and the characteristics of the aggregates with which they are usually associated: a) and b) gel in the interface of the cement and deformed granite (GR2) with subgraining; c) and d) fine cracks in the cement paste (BR2) cutting aggregate of quartzite; e) and f) crack crossing an aggregate particle (AF) with abundant microcrystalline quartz and extending to the cement paste.
Photomicrographs in PPL (a, c and e) and XPL (b, d and f).

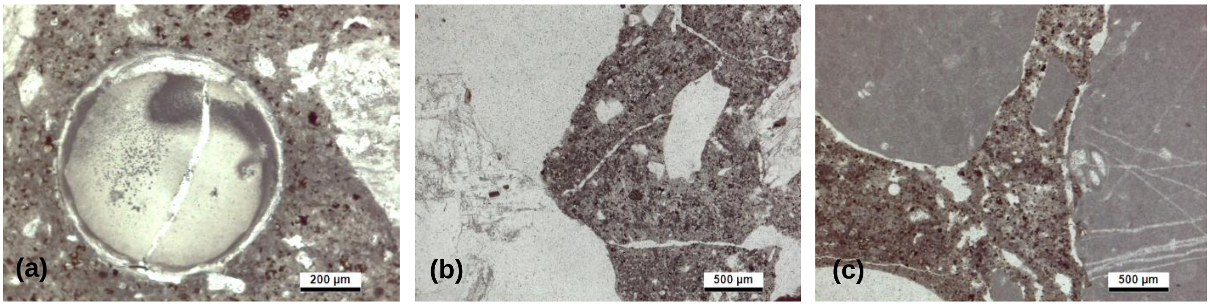

Figure 3.3: AAR features observed in the thin sections of the concrete prisms and which were not considered in the quantification of micro-DRI: a) gel filling a void without cracks in the cement paste (DT1); b) fine cracks in the cement paste that do not show any connection with the aggregate particles (GR5); c) the debonding and pull-outs are artifacts created during the thin section production (CL3).
Photomicrographs in PPL.

3.4 SEM/EDS of ASR products

The alkali-silica gel was characterized by SEM/EDS. Examples of the texture and composition are presented in Figure 3.4. Only amorphous gel was identified in the concrete thin sections. Alkali-silica gel contains Si as the main component. In much lower content there is Ca, K and Na. In some analyses also Al is identified, when there are feldspars close to the cracks filled with gel and, sometimes, close to the cement paste. Usually K is more abundant than Na but both exist is much lower content than Ca. In the cracks that cross the aggregate particles and extend to the cement paste, the content in Ca is higher for gel close to the interface with the cement paste, as also found in [26].

The features observed are similar in all the normally-reactive aggregates (sandstone, tectonite and aggregates with microcrystalline quartz) including the intensely deformed granite samples. The differences are found essentially in the number of cracks and in the amount of gel filling both the cracks and the voids. Following the criteria in [25], the gel in voids was not considered in the micro-DRI quantification. In all these laboratory samples, gel is more abundant in the interfaces between the aggregate particles and the cement paste, forming irregular masses not always related with cracks. Also the appearance of the gel can vary from smooth and colorless, usually in cracks inside the aggregate particles, to brownish, especially in cracks crossing the cement paste. The dense, cracked gel which appears to be in relieve when compared with the surrounding cement paste is not found in deteriorated concrete structures, although the composition is quite similar for the field concrete and the prisms tested in the laboratory.

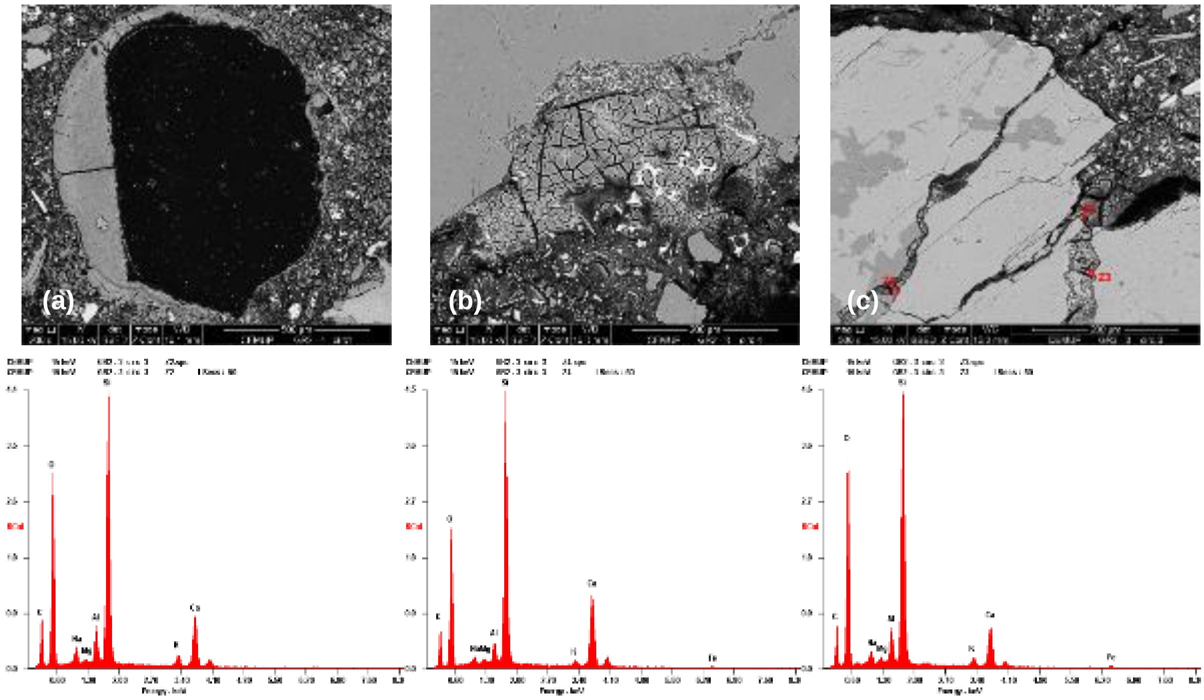

Figure 3.4: SEM images obtained by backscattered electron mode and EDS spectra: gel is dominantly dense and smooth with abundant retraction cracks (might also due to the sample preparation and the use of high vacuum); a) gel partially filling a void (GR2 tested in AAR-4.1);
b) rim of gel in the aggregate/paste interface (GR2 tested in AAR-3); c) gel in the crack inside an aggregate particle (GR2 tested in AAR-4.1). The texture observed in b) is not found in the deteriorated concrete from structures but is quite common in the prisms from the laboratory tests.

4. DISCUSSION

According with the RILEM AAR-0 recommendation [17], for potentially reactive aggregates the petrographic classification must be confirmed by the expansion laboratory tests. When no potentially reactive forms of silica are detected, no further tests are needed. However, in the scope of the research carried out, all the aggregate samples were tested in concrete prism tests AAR-3.1 and AAR-4.1 to verify the correlation between the petrographic classification and the behaviour in concrete exposed to strong adverse conditions. It must be pointed out that granitic rocks without deformation features are usually classified as innocuous but the Portuguese experience makes it mandatory to consider these aggregates of “reactivity uncertain” and to perform CPT’s.

The results presented in Table 3.1 alert to the fact that, for some aggregates, the classification based in the petrographic analysis differs from the expansion obtained in the CPT’s. These discrepancies, as well as the fact that accelerated mortar-bar tests are not adequate for slowly-reactive aggregates [16], are challenging and show that, at least for granitic aggregates, the petrographic analysis might not be enough and a conservative performance of CPTs should be mandatory. The granitic rock masses are characterized by heterogeneous distribution of weathering degree and existence of faults with which fractures and deformation are associated. In this concern, the analysis of representative samples is of upmost importance as the content of deformed rock may vary in volume along the lifetime of the quarry, therefore giving expansion results that might not be consistent over time.

For slowly-reactive aggregates, the expansion results show that AAR-4.1 identifies a larger number of potential reactivity of aggregates than the AAR-3.1 test. From the industry point of view AAR-4.1 is an important test as it is much shorter that the AAR-3.1. However, AAR-3.1 might be more conservative for innocuous aggregates, as observed for BS9.

Concerning the reactive samples, the results confirm that ASR manifestations are related with the presence of microcrystalline quartz in granite *s.l.,* in quartzite/sandstone, in tectonite that occur in the polymictic gravel (BR), and in a strongly deformed meta-rhyolite (DT1) (Figure 3.1). The occurrence of ASR manifestations is mainly dependent on the degree of deformation for the igneous types of aggregates as is demonstrated by comparing the results of concrete manufactured with slowly-reactive aggregates with those with deformed texture e.g. GR2, GR13 and GR18. Regarding the type and content of the ASR manifestations, the behavior of the deformed granitic rocks is similar to that of the natural polymictic gravel, containing sandstone/quartzite and tectonite. The main difference is verified for the intensely deformed meta-rhyolite (DT1) which shows many more cracks crossing aggregate particles than any other of the aggregates analyzed as it is also the aggregate presenting the highest content of micro- to crystalline quartz and producing the highest expansion. In this concern, the comparison between the ASR signs in the concrete prism tests and those observed in field structures demonstrates that in structures the gel in interfaces between the aggregate particles and the cement paste fills cracks and does not form irregular masses, as in CPT (Figure 3.3). Cracks are usually wider and longer in field concrete structures and mostly filled with abundant gel. The occurrence of fibrous to rod-like gel is much more common in ASR affected structures than in the CPT. These characteristics have been discussed in the last decades and further studies are being developed to co-relate the texture and composition of the gel with its potential to cause expansion [11,12]. Apparently, fibrous gel seems to take longer to form than the amorphous gel which may explain why it is usually just incipient to inexistent in CPT.

The results obtained were plotted in charts of correlation between the expansion and the values of micro-DRI (Figure 4.1), considering all the samples for each test, and separately for the normally-reactive and the slowly-reactive aggregates. It can be verified that the correlation is strong only for the normally-reactive aggregates, and is always higher for AAR-3.1 than for AAR-4.1. Surprisingly, the correlation is negative for slowly-reactive aggregates tested in AAR-4.1. This suggests that for these aggregates the time of exposure is more important than the effect of the temperature. DT1 was not included in the AAR-4.1 charts as it was an outlier in the value of expansion which was not followed by the results of concrete petrography, alerting to the representability of the thin sections compared with the dimensions of the concrete prisms tested.

The combination of the petrographic analysis of the aggregates, the results of expansion of the CPT and the observation of the concrete prisms' thin sections suggests the need for a revised classification of the aggregates. This is particularly sensitive for the "uncertain reactivity" for which the petrographic classification might not be enough. Several slowly-reactive samples do not show one or more of the features listed, whist for the normally-reactive aggregates there are always some gel in cracks or in voids. The most interesting examples are highlighted in the following text.

The dolomite sample DL1, which contains clastic quartz and a fibrous mineral that might correspond to chalcedony, associated with chlorite, does not show cracks or gel of any kind and, therefore, it should be classified as innocuous in accordance both with the expansion tests and the concrete petrographic analysis. The samples GR8 and GR10, which textures show no signs of deformation but contain abundant myrmekite and cracks crossing both quartz and feldspar crystals, were classified as slowly-reactive just based on the Portuguese experience and would be innocuous in AAR-1.1. However, both showed expansion values close to that of GR2, which is the reference example of gneissic-granitic texture with abundant subgraining. For these samples, the explanation found is two-folded: the grains of granite included both in the thin sections of aggregate and in the CPT are not representative of the materials present in the quarry and of the particles included in the CPT, which seems to not be plausible; myrmekite and cracks should be considered as contributing to potential reactivity, as already indicated in [27].

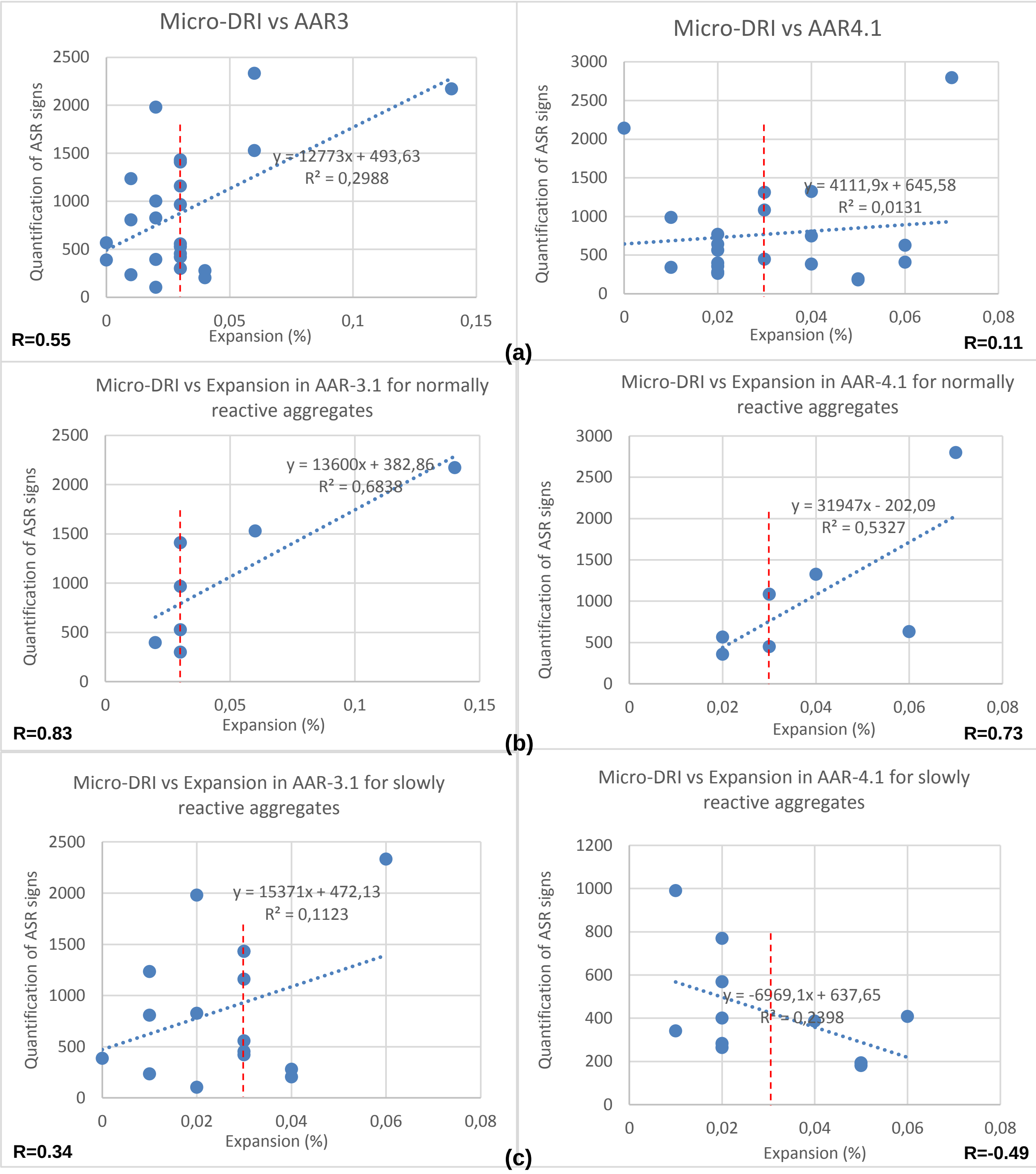

Figure 4.1: Correlation between the values of expansion in AAR-3.1 (left) and AAR-4.1 (right) for: a) all the samples; b) normally reactive; c) slowly-reactive aggregates. In red is the threshold between innocuous and potentially reactive [17]. R is the correlation coefficient (0-0.3 negligible; 0.3-0.5 weak; 0.5-0.7 moderate; 0.7-0.9 strong; >0.9 very strong).

The meta-rhyolite contains abundant cryptocrystalline quartz and the amount of manifestations of ASR proves that this is a normally-reactive aggregate, exhibiting more intense reaction than any of the deformed granites. Also, the micro-DRI obtained for the amphibolite in AAR-4.1 is the highest of all the samples. It can be concluded that the Class II covers a wide range of different textural and/or mineralogical varieties of aggregates and a range of values of expansion. Compared to the results of all the other normally-reactive aggregates, at least the meta-rhyolite should be classified in Class III, although it does not contain opal.

Regarding the correlation between the petrographic classification of the aggregates, the results of expansion and the ASR manifestations, it can be concluded that for the innocuous aggregates the petrographic classification of the aggregate coincides, in general, with both the expansion and the absence of ASR signs. In limestone and dolomite samples there were abundant dark rims in the cement paste around the aggregate particles but no cracks were observed.

The slowly-reactive group of aggregates covers a wide range of lithologies and it was verified that some of them showed variable signs of ASR, e.g. some exhibit gel in voids but no cracks in aggregates or in the cement paste. However, some of the granite samples were rated as reactive both in AAR-3.1 and AAR-4.1 tests, confirming that it is mandatory to lower the content of microcrystalline quartz to classify these aggregates as potentially reactive or even consider as deleterious crystals of quartz that are > 100 µm. Anyway, the results highlight the importance of the representability of the samples and the need to perform concrete expansion tests.

For the normally-reactive aggregates, the results of expansion are higher than for the two previous classes, as expected. All the aggregates in this class are rated as reactive in the AAR-3.1 and AAR-4.1, although the values of expansion were not always followed by the correspondent micro-DRI value.

Table 4.1 summarizes the comparison between the classification based on the petrographic analysis of the aggregates and the micro-DRI results. The classification is made as in [25]. The lower classes of micro-DRI (0-250 and 250-500) only occur for the slowly-reactive samples, whilst the higher rate (≥800) is verified for all the classes of potential reactivity, including 4 of the innocuous aggregates. Also, the manifestations of ASR seem to occur dominantly in the AAR-3.1 test.

Table 4.1: Summary of the results obtained by petrographic analysis of the concrete prims from AAR-3.1 and AAR-4.1 (micro-DRI). Note: the number of thin sections is not equal for both tests.

Petrographic classification of aggregates		Micro-DRI							
		0-250		250-500		500-800		≥800	
[17]	[19]	AAR-3.1	AAR-4.1	AAR-3.1	AAR-4.1	AAR-3.1	AAR-4.1	AAR-3.1	AAR-4.1
Class I	Innocuous				1	2	2	4	1
Class II	Slowly reactive	3	2	4	6	1	2	7	1
	Normally reactive			2	2	1	2	4	3

5. CONCLUSIONS

The assessment of the potential reactivity of Portuguese aggregates followed the national and international recommendations. By using the optical microscope, the aggregates were divided in innocuous, slowly-reactive and normally-reactive, regarding the presence of reactive forms of silica. The most common reactive forms of silica in these aggregates are strained quartz with strain lamellae, subgraining and bulging present in quartzite/sandstone, tectonite and in some granite *s.l.* in tectonites, schists and some dolomite also micro- to cryptocrystalline quartz occurs. There are some discrepancies between the petrographic classification and the expansion results of the innocuous samples, in AAR-3.1 test, and slowly-reactive aggregates, for AAR-4.1 test.

In what concerns the values of expansion, it was concluded that for slowly-reactive rocks the 60 ºC concrete prism test provided more conservative results than those obtained in the traditional 38 ºC CPT.

The most frequent manifestation of ASR in the concrete prisms after the conclusion of the expansion tests is the presence of alkali-silica gel in the paste/aggregate interfaces and gel partially or totally filing voids. Also cracks in the aggregate particles were identified, although more discrete, usually extending to the cement paste. These cracks are empty in the interior of the aggregate particles but contain gel close to the contact with the cement paste and also when cross-cutting the cement paste.

The study suggests that the petrographic analysis of aggregates is a good cost-benefit method for the assessment of reactivity of most of the aggregates but there are exceptions. The most problematic are, however, the slowly-reactive/uncertain reactivity aggregates with a wide variation in the results of the expansion tests. Also, concrete petrography is an effective method for the evaluation of the damage in concrete, revealing that the expansion laboratory tests are quite accurate in the determination of potential reactivity. The use of a micro-DRI parameter shows a very good correlation with the values of expansion in RILEM AAR-3.1 and AAR-4.1 for normally-reactive aggregates but not with slowly-reactive aggregates, with a negative poor correlation in AAR-4.1. The method must be revised and adapted to this scale of observation but it seems to be a good tool for the quantification of manifestations of ASR.

6. ACKNOWLEDGEMENTS

The authors would like to acknowledge the financial support of FCT through the projects UIDB/50019/2020 – IDL and IMPROVE “Improvement of performance of aggregates in the inhibition of alkali-aggregate reactions in concrete” (Ref: PTDC/ECM/115486/2009). We also acknowledge to National Laboratory for Civil Engineering (LNEC) through the project RE-IMPROVE – Expansive Reactions in Concrete – Prevention and mitigation of their effects. The SEM images were performed at CEMUP in an equipment funded by the projects REEQ/1062/CTM/2005 and REDE/1512/RME/2005 of FCT.

7. REFERENCES

[1] Braga Reis, MO, Silva, HS, Santos Silva, A (1996) Alkali-Aggregate Reactions in Portuguese Structures. Some Case Histories, Proceedings of 10th International Conference on Alkali-Aggregate Reaction in Concrete, Melbourne, Australia, pp. 93-100.

[2] Fernandes I, Noronha F, Teles M (2004) Microscopic analysis of alkali-aggregate reaction products in a 50-year-old concrete, Mater Charact 53, Issues 2-4, pp 295-306.

[3] Fernandes I, Noronha F, Teles M (2007) Examination of the concrete from an old Portuguese dam. Texture and composition of alkali-silica gel, Mater Charact 58, Issues 11-12, pp 1160-1170.

[4] Santos Silva A, Gonçalves A (2006) Appendix A – Portugal. In: Wigum BJ, Pedersen LT, Grelk B, Lindġard J (eds.) PARTNER Report 2.1, State-of-the-art report: key parameters influencing the alkali aggregate reaction, SINTEF, Trondheim, Norway, pp. 57–61.

[5] Santos Silva A, Soares D, Matos L, Fernandes I, Salta M (2013) Alkali-aggregate reactions in concrete: Methodologies applied in the evaluation of alkali reactivity of aggregates for concrete. In: A.M.P. Pinto, A.S. Pouzada (eds), Materials Science Forum, Advanced Materials Forum VI, Trans Tech Publications, Switzerland, Chapter 5: Materials for Civil Engineering Applications, 730-732, pp 409-414.

[6] Larive, C, Louarn, N, (1992), Diagnosis of alkali-aggregate reaction and sulphate reaction in French structures, Proceedings of the 9th International Conference on Alkali-Aggregate Reaction, London, July, 1992, 587-598

[7] Fernandes I (2009) Composition of alkali–silica reaction products at different locations within concrete structures. Mater Charact 60, pp 655–668. https://doi.org/10.1016/j.matchar.2009.01.011

[8] Leeman A, Münch B (2019) The addition of caesium to concrete with alkali-silica reaction: Implications on product identification and recognition of the reaction sequence. Cem. Concr. Res. (120), pp 27-35.

[9] Cole WF, Lancucki CJ (1983) Products formed in an aged concrete the occurrence of okenite, Cem. Concr. Res. (13), pp 611–618.

[10] Katayama T (2012) ASR gels and their crystalline phases in concrete – universal products in alkali-silica, alkali-silicate and alkali-carbonate reactions. Proceedings of the 14th International Conference on Alkali-Aggregate Reaction, Austin, USA: 10 pp.

[11] Dähn R, Arakcheeva A, Schaub P, Pattison P, Chapuis G, Grolimund D, Wieland E, Leemann A (2016) Application of micro X-ray diffraction to investigate the reaction products formed by the alkali–silica reaction in concrete structures. Cem. Concr. Res. (79), pp 49-56.

[12] Leemann A (2017) Raman microscopy of alkali-silica reaction (ASR) products formed in concrete. Cem. Concr. Res. (102), pp 41-47.

[13] Katayama T (2010) The so-called alkali-carbonate reaction (ACR) – Its mineralogical and geochemical details, with special reference to ASR. Cem Concr Res. (40), pp 643–675.

[14] Medeiros S, Ramos V, Fernandes I, Nunes JC, Fournier B, Santos Silva A, Soares D (2017) Volcanic aggregates from Azores and Madeira archipelagos (Portugal): an overview regarding the alkali-silica reaction. WMESS conference. IOP Conference Series: Earth and Environmental Science 95 (2017) 022034. DOI:10.1088/1755-1315/95/2/022034.

[15] Ramos V, Fernandes I, Noronha F, Katayama T, Soares D, Santos Silva A (2014) Potential Reactivity to Alkalis of Portuguese Volcanic Aggregates for Concrete", In: G. Lollino, A. Manconi, F. Guzzetti, M. Culshaw, P. Bobrowsky, F. Luino (Editors) IAEG XII Congress 2014 Engineering Geology for Society and Territory. Volume 5, Urban Geology, Sustainable Planning and Landscape Exploitation, Springer, pp 55-58. Torino.

[16] Ramos V, Fernandes I, Noronha F, Santos Silva A, Soares D, Leal S, Fournier B (2016) Assessment of the potential reactivity of granitic rocks. Petrography and expansion tests. Cem. Concr. Res. (86), pp 63–77. https://doi.org/10.1016/j.cemconres.2016.05.001

[17] Nixon PJ and Sims I (2016) RILEM Recommendations for the prevention of damage by alkali-aggregate reactions in new concrete structures. State-of-the-Art Report of the RILEM Technical Committee 219-ACS. RILEM State-of-the-Art Reports 17, pp. 176.

[18] LNEC E 461 (2007). Betões. Metodologias para prevenir reacções expansivas internas. Especificação LNEC, Lisboa, Portugal (6 pp in Portuguese).

[19] Lindgård J, Nixon PJ, Borchers I, Schouenborg B, Wigum BJ, Haugen M, Åkesson U (2010) The EU "PARTNER" Project - European standard tests to prevent alkali reactions in aggregates: final results and recommendations. Cem. Concr. Res. (40), pp 611-635. https://doi.org/10.1016/j.cemconres.2009.09.004

[20] Lindgård J, Andiç-Çakır O, Fernandes I, Thomas MDA, Rønning TF (2012) Alkali-silica reactions (ASR): literature review on parameters influencing laboratory performance testing, Cem. Concr. Res. (42), pp 223–243.

[21] Fernandes I, Ribeiro MA, Martins HCB, Noronha F, Soares D, Santos Silva A, Broekmans MATM, Sims I (2016) To be or not to be... alkali-reactive. A challenge for the petrographic method. In: Bernardes HM, Hasparyk NP (eds), Proc 15th ICAAR - International Conference on Alkali-Aggregate Reactions in Concrete, S. Paulo, Brazil, 10 pp.

[22] Fernandes I, Ribeiro MA, Broekmans MATM, Sims I (Eds) (2016) Petrographic Atlas. Characterisation of aggregates regarding potential reactivity to alkalis. RILEM TC 219-ACS Recommended Guidance AAR-1.2, for use with the RILEM AAR-1.1 Petrographic Examination Method, Springer, 193 pp. DOI: 10.1007/978-94-017-7383-6.

[23] EN 197-1 (2000) Cement - Part 1: Composition, specifications and conformity criteria for common cements, CEN.

[24] Poole AB, Sims I (2015) Concrete petrography. A handbook of investigative techniques. Second Edition. Taylor & Francis, CCR Press, USA.

[25] Sanchez LFM, Fournier B, Jolin M; Duchesne J (2015) Reliable Quantification of AAR Damage Through Assessment of the Damage Rating Index (DRI)," Cement and Concrete Research 67, pp. 74-92.

[26] Leemann A, Katayama T, Fernandes I, Broekmans MA (2016) Types of alkali–aggregate reactions and the products formed, Proc. Inst. Civil Eng. Constr. Mater. 169, pp 128–135.

[27] Wigum BJ (1995) Examination of microstructural features of Norwegian cataclastic rocks and their use for predicting alkali-reactivity in concrete, Eng. Geol. 40, pp. 195–214.